THE ASTROPHYSICAL JOURNAL, 522:L39–L42, 1999 September 1

BVRI OBSERVATIONS OF THE OPTICAL AFTERGLOW OF GRB 990510[1]

K. Z. STANEK[2] AND P. M. GARNAVICH
Harvard-Smithsonian Center for Astrophysics, 60 Garden Street, MS20, Cambridge, MA 02138;
kstanek@cfa.harvard.edu, peterg@cfa.harvard.edu
J. KALUZNY[2] AND W. PYCH
Warsaw University Observatory, Al. Ujazdowskie 4, PL-00-478 Warszawa, Poland;
jka@sirius.astrouw.edu.pl, pych@sirius.astrouw.edu.pl
AND
I. THOMPSON
Carnegie Observatories, 813 Santa Barbara Street, Pasadena, CA 91101-1292; ian@ociw.edu
Received 1999 May 26; accepted 1999 July 1; published 1999 July 21

ABSTRACT

We present *BVRI* observations of the optical counterpart to GRB 990510 obtained with the Las Campanas 1.0 m telescope between 15 and 48 hr after the burst. The temporal analysis of the data indicates steepening decay, independent of wavelength, approaching asymptotically $t^{-0.76\pm0.01}$ at early times ($t \ll 1$ day) and $t^{-2.40\pm0.02}$ at late times, with the break time at $t_0 = 1.57 \pm 0.03$ days. GRB 990510 is the most rapidly fading of the well-documented gamma-ray burst (GRB) afterglows. It is also the first well-observed example of a broadband break for a GRB optical counterpart. The optical spectral energy distribution, corrected for significant Galactic reddening, is well fitted by a single power law with $\nu^{-0.61\pm0.12}$. However, when the *B*-band point is dropped from the fit, the power law becomes $\nu^{-0.46\pm0.08}$, indicating a possible deviation from the power law in the spectrum, either intrinsic or due to additional extinction near the source or from an intervening galaxy at $z = 1.62$. Broadband break behavior broadly similar to that observed in GRB 990510 has been predicted in some jet models of GRB afterglows, thus supporting the idea that the GRB energy is beamed, at least in some cases.

Subject heading: gamma rays: bursts

1. INTRODUCTION

The *BeppoSAX* satellite (Boella et al. 1997) has brought a new dimension to gamma-ray burst (GRB) research by rapidly providing good localization of several bursts per year. This has allowed many GRBs to be followed up at other wavelengths, including X-ray (Costa et al. 1997), optical (van Paradijs et al. 1997), and radio (Frail et al. 1997). Good positions have also allowed redshifts to be measured for a number of GRBs (e.g., GRB 970508: Metzger et al. 1997), providing a definite proof for their cosmological origin.

GRB 990510 was detected by *BeppoSAX* (Piro et al. 1999) on May 10.36743 UT, and the fluence was among the highest of the *BeppoSAX* localized events, after GRB 990123, GRB 980329, and GRB 970111 (Amati et al. 1999). It was also detected by BATSE (Kippen et al. 1999), and its peak flux and fluence rank it in the top 4% (9%) of BATSE burst flux (fluence) distributions. The *BeppoSAX* NFI follow-up of GRB 990510 started about 8 hr after the burst (Kuulkers et al. 1999) and detected a strong X-ray afterglow.

Axelrod, Mould, & Schmidt (1999) were the first to optically monitor the field of GRB 990510, starting on 10.514 UT, i.e., only 3.5 hr after the burst, using the Mount Stromlo 50 inch (127 cm) telescope. The optical counterpart to GRB 990510 was first identified by Vreeswijk et al. (1999a) with data taken about 8.5 hr (May 10.73 UT) after the burst using the Sutherland 1.0 m telescope. It was easily recognized as a bright ($R \approx 18.5$), new object not present in the Digitized Sky Survey image at the position of $\alpha = 13^{h}38^{m}07^{s}.64$, $\delta = -80°29'48''.8$ (J2000.0) (Kaluzny et al. 1999b). Galama et al. (1999) confirmed the optical transient (OT) with the ESO 2.2 m telescope on May 10.99 UT and found it to be declining with a temporal decay index of -0.85. Kaluzny et al. (1999a, 1999b) observed GRB 990510 with the Las Campanas 1.0 m telescope beginning on May 10.995 and found that the object declined by 0.34 mag in the *R* band over 4.6 hr. Absorption lines at $z = 1.619$ seen in the optical spectrum of GRB 990510 taken with the Very Large Telescope Unit 1 8 m telescope by Vreeswijk et al. (1999b) provide a lower limit to the redshift of the GRB source.

By adding data taken during their second night (starting May 12.0 UT), Stanek et al. (1999) noticed the steepening of the OT decline, and they derived a power-law decay index of -1.36 by a fit to their data from both nights, but they also showed that a single power law does not provide a good fit to all the data. Analysis of more data has confirmed this behavior (Hjorth et al. 1999; Bloom et al. 1999; Marconi et al. 1999a). We will discuss in detail the temporal behavior of the GRB 990510 OT further in this Letter.

We describe the data and the reduction procedure in § 2. In § 3 we discuss the multiband temporal behavior of the GRB OT. In § 4 we describe the broadband spectral properties of the afterglow deduced from our optical data.

2. THE DATA AND THE REDUCTION PROCEDURE

The data were obtained with the Las Campanas Observatory 1.0 m Swope telescope on two nights, 1999 May 10/11 and May 11/12 UT. We used the backside-illuminated SITE3 2048 × 4096 CCD, with the pixel scale of $0''.44$ pixel^{-1}. To speed up the readout time we used only a 2048 × 1200 section of the CCD. We have obtained 35 *R*-band, 20 *V*-band, 16 *I*-band, and four *B*-band images, with exposure times ranging from 240 s during the first night to 900 s during the second

[1] Based on the observations collected at the Las Campanas Observatory 1 m Swope telescope.
[2] Also at N. Copernicus Astronomical Center, Bartycka 18, Warszawa PL-00-716, Poland.

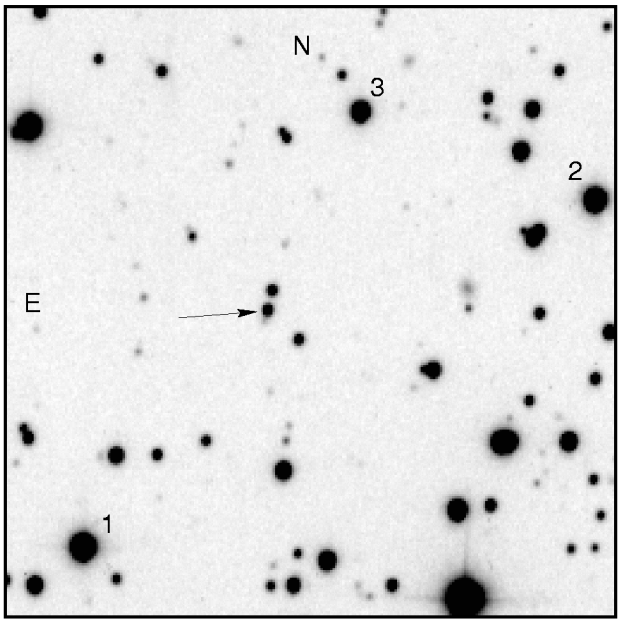

FIG. 1.—Finding chart for the field of GRB 990510. The optical transient is indicated with an arrow. Also shown are the three comparison stars calibrated by Pietrzyński & Udalski (1999a, 1999b) and Bloom et al. (1999).

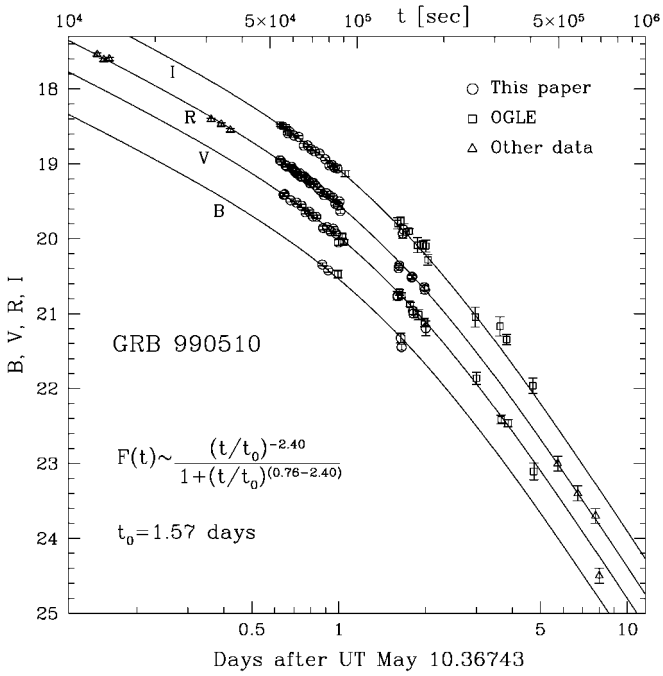

FIG. 2.—*BVRI* light curves of GRB 990510. Our data is shown with circles and OGLE data with squares. Other data used to constrain the fits is shown with triangles (for references see text). Also shown is the simple analytical fit discussed in the text.

night.[3] The image quality was good, with median seeing for the *R*-band of 1.″4. The finding chart for GRB 990510 is shown in Figure 1.

The data were reduced using two different methods. First, we have used the photometric data pipeline of the DIRECT project (Kaluzny et al. 1998; Stanek et al. 1998), which is based on the DAOPHOT point-spread function–fitting image reduction package (Stetson 1987, 1992). To check the consistency of the differential photometry, we have also employed the image subtraction method of Alard & Lupton (1998) and Alard (1999) as implemented in the ISIS image subtraction package (C. Alard 1999, private communication[4]). We have found very good agreement between these two data reduction methods (rms scatter of 0.013 mag).

The calibration for the field has been obtained by Pietrzyński & Udalski (1999a, 1999b) in the *BVI* bands and by Bloom et al. (1999) in the *VR* bands. In both cases the quoted uncertainty of the calibration zero point is ± 0.03 mag for the *VRI* bands and ± 0.05 mag for the *B* band. Comparison of the *V*-band measurements for three secondary standards given by Pietrzyński & Udalski (1999a, 1999b) and Bloom et al. (1999) in the GRB field yields a systematic difference of 0.025 mag, i.e., within the quoted uncertainty. We have adopted the calibration of Pietrzyński & Udalski (1999a, 1999b) for the *BVI* bands and the calibration of Bloom et al. (1999) for the *R* band.

3. THE TEMPORAL BEHAVIOR

We plot the GRB 990510 *BVRI* light curves in Figure 2. Most of the data come from our monitoring (Kaluzny et al. 1999a, 1999b; Stanek et al. 1999) and from the Optical Gravitational Lensing Experiment (OGLE) project (Pietrzyński & Udalski 1999a, 1999b, 1999c). We use those OGLE points that extend the time coverage beyond that of our data. In addition, we use the early *R*-band data of Axelrod et al. (1999) and Galama et al. (1999), later *R*-band data points of Marconi et al. (1999a, 1999b), and one late *V*-band point obtained by Beuermann, Reinsch, & Hessman (1999). All these data extend beyond our time coverage and are therefore useful for constraining the time evolution of the afterglow.

As noticed by Stanek et al. (1999) using data from 2 days only, the optical *R*-band data already showed clear departure from the initial shallow power law of about -0.9 determined by Galama et al. (1999) and Kaluzny et al. (1999a, 1999b) from the first day data. This trend of steepening decay was confirmed later by Hjorth et al. (1999) and others.

To describe the temporal evolution of the GRB 990510 optical counterpart, we use the combined data described earlier and fit to each *VRI* band separately the following four-parameter formula (similar to that of Bloom et al. 1999 and Marconi et al. 1999a):

$$F_\nu(t) = \frac{k_\nu\,(t/t_0)^{-a_1}}{1 + (t/t_0)^{(a_2-a_1)}}\,, \qquad (1)$$

where k_ν is a normalization constant specific for each band such that the magnitude is given by $m(t) = \text{const} - 2.5 \log (F_\nu)$. This formula describes power-law t^{-a_2} decline at early times ($t \ll t_0$) and another power-law t^{-a_1} decline at late times ($t \gg t_0$). The total number of points used for the fits was 44 for the *R* band, 32 for the *V* band, 31 for the *I* band, and five for the *B* band, for a total of 112 points. The *R*-band data have the most extensive temporal coverage, especially early after the burst. The other bands are not as well constrained, at least with the data at hand, which demonstrates the importance of getting multiband follow-up images as early as possible. The parameters are correlated with each other, so we first fit the *R* band

[3] *BVRI* data are available through anonymous ftp on cfa-ftp.harvard.edu, in pub/kstanek/GRB990510 directory and through the World Wide Web at http://cfa-www.harvard.edu/cfa/oir/Research/GRB/.

[4] See http://www.iap.fr/users/alard/package.html.

TABLE 1
GRB 990510 BEST-FIT PARAMETERS

Band	a_1	a_2	t_0 (days)	χ^2/dof
R	2.41 ± 0.02	0.76 ± 0.01	1.55 ± 0.03	1.51
V	2.46 ± 0.05	0.73 ± 0.02	...	1.22
I	2.17 ± 0.07	0.82 ± 0.04	...	1.03
BVRI	2.40 ± 0.02	0.76 ± 0.01	1.57 ± 0.03	1.48

and then use the derived t_0 value as fixed for the *VI* bands. We also run a combined fit to all *BVRI* data, requiring the same a_1, a_2, t_0 for all four bands, but allowing a different normalization constant for each band. The results of this combined fit are shown as the continuous lines in Figure 2, and the best-fit parameters for all the fits are presented in Table 1. The errors shown are based on conditional probability distributions, fixing two of the parameters at their most probable values.

The combined fit does a good job of representing the overall temporal behavior of the *BVRI* data set, but it is clearly dominated by the *R*-band data. Considering that these data represent an inhomogeneous data set, the χ^2/degree of freedom (dof) values for the *VI* bands are rather good. The χ^2/dof is somewhat higher for the *R* band. Since our *R*-band data have somewhat better photometric accuracy than the *VI* data, this might indicate that we see some small, short-timescale departures from the analytical fit. Our frequent observations of the GRB optical counterpart during the first night were obtained to test for such rapid variations. After we subtract the long-term trend derived above, we get an rms scatter of 0.021 mag, with the largest deviation of 0.08 mag. Comparing to constant field stars with similar magnitude, the observed scatter is consistent with photometric noise. Clearly, brightness variations on timescales from 0.1 to 2 hr are small. We note that Hjorth et al. (1999) obtained similar rms scatter in their 31 300 s *R*-band images, obtained with the 1.54 m telescope on La Silla at times overlapping with our observations. By combining these two data sets, one might be able to search with more sensitivity for correlated variations in the brightness of the afterglow.

4. REDDENING AND BROADBAND SPECTRAL ENERGY DISTRIBUTION

GRB 990510 is located at Galactic coordinates of $l = 304\overset{\circ}{.}9426$, $b = -17\overset{\circ}{.}8079$. To remove the effects of the Galactic interstellar extinction, we used the reddening map of Schlegel, Finkbeiner, & Davis (1998, hereafter SFD). As noticed by Stanek (1999), the expected Galactic reddening toward the burst is significant, $E(B-V) = 0.203$, which corresponds to expected values of Galactic extinction $A_B = 0.88$, $A_V = 0.66$, $A_R = 0.53$, and $A_I = 0.40$ for the Landolt (1992) Cerro Tololo Inter-American Observatory filters and standard reddening curve of Cardelli, Clayton, & Mathis (1989).

We synthesize the *BVRI* energy distribution from our data by interpolating the magnitudes to a common time. As discussed in the previous section, the optical colors of the GRB 990510 counterpart do not show significant variation. We therefore select an epoch of May 11.26 UT (21.5 hr after the burst) for the color analysis, which coincides with our first *B*-band images. Using the all-band fit from the previous section, we get for this epoch $B_{21.5} = 20.39 \pm 0.05$, $V_{21.5} = 19.82 \pm 0.03$, $R_{21.5} = 19.40 \pm 0.03$, and $I_{21.5} = 18.93 \pm 0.03$, where the 0.03 mag error bar represents the combined uncertainty in the zero-point calibration and the small measurement errors. Using the SFD extinction values, this translates to unreddened values of $B_{0,21.5} = 19.51 \pm 0.10$, $V_{0,21.5} = 19.16 \pm 0.07$, $R_{0,21.5} = 18.87 \pm 0.06$, and $I_{0,21.5} = 18.53 \pm 0.05$ [following SFD, we took the error in $E(B-V)$ to be 0.02 mag]. It is outside the scope of this Letter to discuss properly the systematic errors of the SFD map, but there is some indication that it overestimates the $E(B-V)$ values by a factor of 1.3–1.5 close to the Galactic plane ($|b| < 5°$) (Stanek 1998) and in high extinction ($A_V > 0.5$ mag) regions (Arce & Goodman 1999). It is not clear at all that such a correction should be applied to the SFD $E(B-V)$ value for GRB 990510, but it would reduce this value to about $E(B-V) = 0.15$.

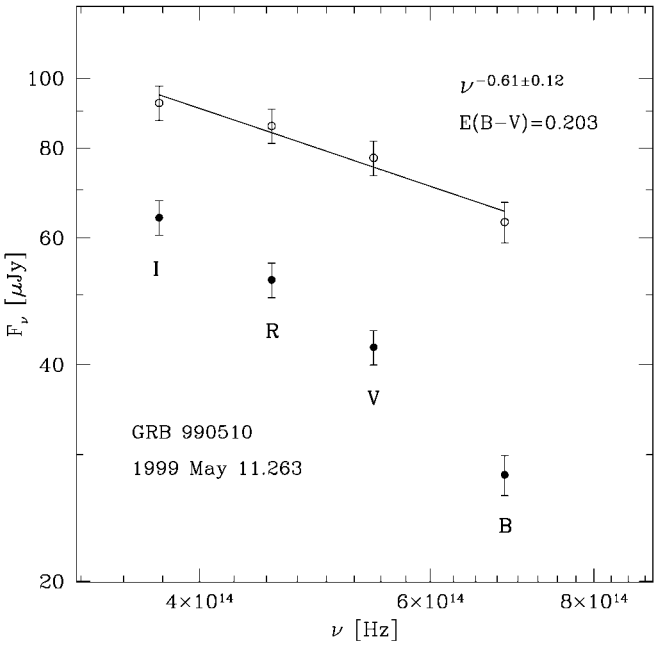

FIG. 3.—Synthetic energy distribution of GRB 990510 21.5 hr after the burst, constructed using analytical fit shown in Fig. 2.

We convert the *BVRI* magnitudes to fluxes using the effective wavelengths and normalizations of Fukugita, Shimasaku, & Ichikawa (1995). These conversions are accurate to about 5%, which increases the error bars correspondingly. Note that while the error in the $E(B-V)$ reddening value has not been applied to the error bars of individual points, we include it in the error budget of the fitted slope. The results are plotted in Figure 3 for both the observed and the dereddened magnitudes. The spectrum is well fitted by a single power law with $\nu^{-0.61\pm0.12}$, although when the *B*-band point is dropped from the fit, the power law becomes $\nu^{-0.46\pm0.08}$. The shift in the index when the *B* band is removed suggests a possible deviation from the power law in the blue part of the spectrum. This is either intrinsic to the spectrum or due to additional extinction somewhere along the line of sight. If we use the value of $E(B-V) = 0.15$, the corresponding numbers are $\nu^{-0.80\pm0.12}$ for all the bands and $\nu^{-0.63\pm0.09}$ without the *B*-band point.

It might be interesting to ask how much more reddening would be required to produce the same power law with and without the *B*-band point. Doubling the amount of Galactic reddening to $E(B-V) = 0.406$ produces $\nu^{0.10\pm0.08}$ for all the bands and $\nu^{0.17\pm0.09}$ without the *B*-band point.

5. CONCLUSIONS

We presented *BVRI* observations of GRB 990510. Our analysis of the data indicates steepening decay, independent of

optical wavelength, with power-law behavior $t^{-0.76\pm0.01}$ at early times ($t \ll 1$ day) and second power-law $t^{-2.40\pm0.02}$ at late times and with the break time at $t_0 = 1.57 \pm 0.03$ days. This is the first well-observed example of such a broadband break for a GRB OT, and it is very well documented thanks to a concerted effort by the astronomical community. We would like to stress the importance of multiband optical observations for GRB studies, especially early after the burst. This allows for much better constraint of the GRB multiband temporal behavior, which is especially important if the broadband break happens early after the burst.

The optical spectral energy distribution, corrected for significant Galactic reddening, is well fitted by a single power law with $\nu^{-0.61\pm0.12}$. However, when the *B*-band point is dropped from the fit, the power law becomes $\nu^{-0.46\pm0.08}$, indicating a possible deviation from the power law in the spectrum, either intrinsic or due to additional extinction near the host or at the intervening galaxy at $z = 1.62$.

The temporal behavior of GRB 990510 is broadly similar to predictions of GRB jet models (Rhoads 1999). A break in the light curve is expected when the jet makes the transition to sideways expansion after the relativistic Lorentz factor drops below the inverse of the opening angle of the initial beam. After the break, the temporal power-law index is expected to approach the electron energy distribution index with values between 2.0 and 2.5, which is consistent with the late-time decline observed here for GRB 990510 (Halpern et al. 1999; Sari, Piran, & Halpern 1999). However, the early-time decay index and the spectral slope of GRB 990510 are not as well explained by the models. The clear break seen in the multicolor light curves of GRB 990510 provides the first direct evidence that, in some cases, GRB energy is not ejected isotropically.

S. Barthelmy, the organizer of the GRB Coordinates Network (GCN), is recognized for his extremely useful effort. The OGLE collaboration is thanked for making their data promptly available to the astronomical community. We thank C. Alard for his support with the ISIS image subtraction package. We thank B. Paczyński and L. A. Phillips for useful discussions and comments on the Letter. K. Z. S. was supported by the Harvard-Smithsonian Center for Astrophysics Fellowship. J. K. was supported by NSF grant AST 95-28096 to B. Paczyński and by the Polish KBN grant 2P03D011.12. W. P. was supported by the Polish KBN grant 2P03D010.15.

REFERENCES

Alard, C. 1999, A&A, in press (astro-ph/9903111)
Alard, C., & Lupton, R. H. 1998, ApJ, 503, 325
Amati, L., et al. 1999, GCN Circ. 317 (http://gcn.gsfc.nasa.gov/gcn/gcn3/317.gcn3)
Arce, H. G., & Goodman, A. A. 1999, ApJ, 512, L135
Axelrod, T., Mould, J., & Schmidt, B. 1999, GCN Circ. 315 (http://gcn.gsfc.nasa.gov/gcn/gcn3/315.gcn3)
Beuermann, K., Reinsch, K., & Hessman, F. V. 1999, GCN Circ. 331 (http://gcn.gsfc.nasa.gov/gcn/gcn3/331.gcn3)
Bloom, J. S., et al. 1999, GCN Circ. 323 (http://gcn.gsfc.nasa.gov/gcn/gcn3/323.gcn3)
Boella, G., et al. 1997, A&AS, 122, 299
Cardelli, J. A., Clayton, G. C., & Mathis, J. S. 1989, ApJ, 345, 245
Costa, E., et al. 1997, Nature, 387, 78
Frail, D. A., Kulkarni, S. R., Nicastro, L., Feroci, M., & Taylor, G. B. 1997, Nature, 389, 261
Fukugita, M., Shimasaku, K., & Ichikawa, T. 1995, PASP, 107, 945
Galama, T. J., et al. 1999, GCN Circ. 313 (http://gcn.gsfc.nasa.gov/gcn/gcn3/313.gcn3)
Halpern, J. P., Kemp, J., Piran, T., & Bershady, M. A. 1999, ApJ, 517, L105
Hjorth, J., et al. 1999, GCN Circ. 320 (http://gcn.gsfc.nasa.gov/gcn/gcn3/320.gcn3)
Kaluzny, J., Garnavich, P. M., Stanek, K. Z., Pych, W., & Thompson, I. 1999a, GCN Circ. 314 (http://gcn.gsfc.nasa.gov/gcn/gcn3/314.gcn3)
———. 1999b, IAU Circ. 7164
Kaluzny, J., Stanek, K. Z., Krockenberger, M., Sasselov, D. D., Tonry, J. L., & Mateo, M. 1998, AJ, 115, 1016
Kippen, R. M., et al. 1999, GCN Circ. 322 (http://gcn.gsfc.nasa.gov/gcn/gcn3/322.gcn3)
Kuulkers, E., et al. 1999, GCN Circ. 326 (http://gcn.gsfc.nasa.gov/gcn/gcn3/326.gcn3)
Landolt, A. 1992, AJ, 104, 340
Marconi, G., et al. 1999a, GCN Circ. 329 (http://gcn.gsfc.nasa.gov/gcn/gcn3/329.gcn3)
———. 1999b, GCN Circ. 332 (http://gcn.gsfc.nasa.gov/gcn/gcn3/332.gcn3)
Metzger, M. R., et al. 1997, Nature, 387, 879
Pietrzyński, G., & Udalski, A. 1999a, GCN Circ. 316 (http://gcn.gsfc.nasa.gov/gcn/gcn3/316.gcn3)
———. 1999b, GCN Circ. 319 (http://gcn.gsfc.nasa.gov/gcn/gcn3/319.gcn3)
———. 1999c, GCN Circ. 328 (http://gcn.gsfc.nasa.gov/gcn/gcn3/328.gcn3)
Piro, L., et al. 1999, GCN Circ. 304 (http://gcn.gsfc.nasa.gov/gcn/gcn3/304.gcn3)
Rhoads, J. E. 1999, ApJ, submitted (astro-ph/9903399)
Sari, R., Piran, R., & Halpern, J. P. 1999, ApJ, 519, L17
Schlegel, D. J., Finkbeiner, D. P., & Davis, M. 1998, ApJ, 500, 525 (SFD)
Stanek, K. Z. 1998, preprint (astro-ph/9802307)
———. 1999, GCN Circ. 312 (http://gcn.gsfc.nasa.gov/gcn/gcn3/312.gcn3)
Stanek, K. Z., Garnavich, P. M., Kaluzny, J., Pych, W., & Thompson, I. 1999, GCN Circ. 318 (http://gcn.gsfc.nasa.gov/gcn/gcn3/318.gcn3)
Stanek, K. Z., Kaluzny, J., Krockenberger, M., Sasselov, D. D., Tonry, J. L., & Mateo, M. 1998, AJ, 115, 1894
Stetson, P. B. 1987, PASP, 99 191
———. 1992, in ASP Conf. Ser. 25, Astrophysical Data Analysis Software and Systems I, ed. D. M. Worrall, C. Bimesderfer, & J. Barnes (San Francisco: ASP), 297
van Paradijs, J., et al. 1997, Nature, 386, 686
Vreeswijk, P. M., et al. 1999a, GCN Circ. 310 (http://gcn.gsfc.nasa.gov/gcn/gcn3/310.gcn3)
———. 1999b, GCN Circ. 324 (http://gcn.gsfc.nasa.gov/gcn/gcn3/324.gcn3)